# Sub-kilohertz linewidth free-running monolithic cavity VECSEL with $10^{-12}$ stability ⬤

P. H. Moriya ✉ iD ; M. Lee iD ; J. E. Hastie iD

Check for updates

View Online    Export Citation

# Sub-kilohertz linewidth free-running monolithic cavity VECSEL with $10^{-12}$ stability (F)

P. H. Moriya,[a] (iD) M. Lee, (iD) and J. E. Hastie (iD)

**AFFILIATIONS**

Institute of Photonics, Department of Physics, SUPA, University of Strathclyde, Technology and Innovation Centre, 99 George Street, Glasgow G1 1RD, United Kingdom

[a]Author to whom correspondence should be addressed: paulo.moriya@strath.ac.uk

**ABSTRACT**

We report the development of a compact, highly stable, monolithic-cavity, GaInP/AlGaInP-based vertical-external-cavity surface-emitting laser (VECSEL) with electronically tunable emission wavelength centered at 689.4425 nm for neutral strontium (Sr)-based applications. The output power reaches 40 mW (pump-power-limited) with ultra-low frequency and intensity noise performance resulting in a free-running linewidth of 720 Hz, reduced to 390 Hz when frequency locked to a reference cavity and verified via a heterodyne beat note measurement with 2 s averaging time. For shorter averaging times (0.1 ms), the free-running linewidth is as low as 40 Hz. We estimate a Lorentzian, or intrinsic, linewidth of 64 mHz from the frequency noise power spectral density at high frequencies, thus providing further evidence of the ultra-narrow fundamental linewidth of VECSELs. High frequency stability was measured via Allan deviation resulting in $1.05 \times 10^{-12}$ at 2 s and $2.11 \times 10^{-13}$ at 7 s averaging times when the 689 nm monolithic cavity VECSEL is free-running and locked, respectively, suitable for neutral Sr-based quantum technologies, such as optical clocks and atom interferometry.

Ultra-low noise and highly coherent lasers are a critical part of the so-called quantum technologies (QT), such as optical clocks[1] and atom interferometers,[2] being responsible for the creation and manipulation of quantum matter, with direct effect on the overall efficiency and accuracy of the QT system. For example, neutral strontium (Sr) optical clocks require blue and red lasers with different brightness and linewidth to target the singlet and triplet transitions, respectively, for the production of ultra-cold atomic clouds.[3,4] The linewidth requirements are more challenging at the red wavelengths where lasers at 689 nm, with kilohertz, and at 698 nm, with sub-hertz, spectral widths are required to address the neutral Sr second cooling and clock transitions, respectively. External cavity diode lasers (ECDLs)[5] and solid-state lasers (SSLs)[6] are commonly employed for this kind of application but with limited short wavelength coverage, especially in the visible part of the electromagnetic spectrum, and with low brightness, thus limiting the number of atomic, molecular, and ionic species that can be exploited. In addition, these laser technologies have Schawlow–Townes–Henry (STH), or fundamental, linewidth limits[7,8] of kilohertz or greater, which is then broadened by environmental, thermal, mechanical, and electronic noise leading to free-running linewidths at the 100 kHz-level, thus preventing access to narrow atomic

transitions directly without complex frequency, intensity, and/or phase stabilization stages. These extra modules, including those for power scaling and beam profile correction, that are required to meet the desired laser performance, have direct impact not only on the QT system bulk, complexity, and portability, but also reduce or prevent deployment capability for field trials.

Other laser technologies, such as vertical-external-cavity surface-emitting lasers (VECSELs)—also known as semiconductor disk lasers (SDLs)—have been explored as an attractive alternative given their high brightness, extended wavelength coverage, and relaxation-oscillation-free (so-called class-A[9]) low-noise performance while having STH limits at the millihertz-level.[10] This allowed us to demonstrate low noise operation with sub-kilohertz linewidth of actively stabilized, air-spaced cavity GaInP/AlGaInP-based VECSELs at 689 (Ref. 11) and 698 (Ref. 12) nm, the wavelengths required to target the red laser cooling and clock transitions of neutral Sr atoms, with output power exceeding 100 mW. More recently, to significantly reduce the impact of environmental noise, we have introduced the concept of monolithic cavity architectures, used, e.g., in nonplanar ring oscillator (NPRO) lasers,[13] to class-A VECSELs. The monolithic cavity VECSEL was formed by a total internal reflection laser resonator created inside a

right-angle prism, thus producing a wavelength customizable, high stability, class-A laser platform for high precision applications,[14] in this case oscillating at 672 nm with an output power of 19 mW and a free-running linewidth of 1.9 kHz for a sampling time of 1 s.

In this article, we report the achievement of sub-kilohertz free-running linewidth of a green-diode-pumped, monolithic cavity AlGaInP-based VECSEL with output power reaching 40 mW at an emission wavelength of 689.4425 nm[15] to target the second cooling transition of neutral Sr atoms. We also introduce frequency-locking of the monolithic resonator via a bonded shear piezoelectric transducer. Low relative intensity and frequency noise were observed with a free-running linewidth of 720 Hz, reduced to 390 Hz when frequency-locked to a moderately high finesse reference cavity via the Pound–Drever–Hall technique,[16] measured via a heterodyne beat note against an independent air-spaced cavity, narrow linewidth red VECSEL system. Furthermore, the frequency stability of the monolithic laser was measured via Allan deviation to be $1.05 \times 10^{-12}$ (2 s) and $2.11 \times 10^{-13}$ (7 s) while free-running and locked, respectively, suitable for high performance applications, such as QT and metrology. Finally, the ultra-narrow Lorentzian, or intrinsic, linewidth was estimated to be 64 mHz for the VECSEL presented here, which is still orders of magnitude lower than that being demonstrated for hybrid and heterogeneously integrated semiconductor lasers.[17–19] In conjunction with a compact, intensity-stabilized green diode pump, this low noise VECSEL architecture has the potential to reduce even further the laser system bulk and complexity, and an even narrower linewidth moving toward the VECSEL fundamental limit, with an overall stability suitable for QT and metrology.

The monolithic cavity VECSEL resonator Is formed inside an off-the-shelf, 25 mm, fused silica right-angle prism,[14] see Figs. 1(a) and 1(b). The laser mode is folded twice via the total internal reflection between the distributed Bragg reflector (DBR) of the gain structure and a 1% planar-convex output coupler, both capillary-bonded to the hypotenuse surface of the prism with reasonably high tolerance of the transverse alignment (> mm), given the 4-mm width of the uniform gain structure. An AlGaInP-based VECSEL gain structure, similar to that reported in the literature by our group,[11] was selected for emission at 689 nm when optically pumped at green wavelengths, being formed of compressively strained GaInP quantum wells, grouped in pairs, separated by AlGaInP barrier layers for resonant periodic gain (RPG), grown on top of a high reflectivity (>99.99%) AlGaAs/AlAs distributed Bragg reflector (DBR) mirror on a GaAs substrate [see Fig. 1(c)]. First, the VECSEL sample is capillary-bonded to a crystalline heatspreader for thermal management, and then, optical contact bonding is used for securing the sample and heatspreader to the prism, which is then placed in a brass mount, temperature-stabilized at 18 °C (tunable between 10 and 30 °C with sub-mK precision). A shear piezoelectric transducer (PZT) is mounted on the top of the right-angle prism for wavelength tuning and frequency stabilization. Finally, an intensity-stabilized, green diode laser is used as an optical pump,[20] with a maximum power of 1050 mW delivered to the gain structure via a multimode fiber and f = 50 mm lens through one of the lateral faces of the prism (coupling efficiency = 85% and focus spot size diameter ∼61 μm).

Single frequency emission with a pump-power-limited maximum output power of 40 mW at 689.4425 nm is achieved, with a threshold of 630(20) mW and a conversion efficiency of 8.4(1)% [see
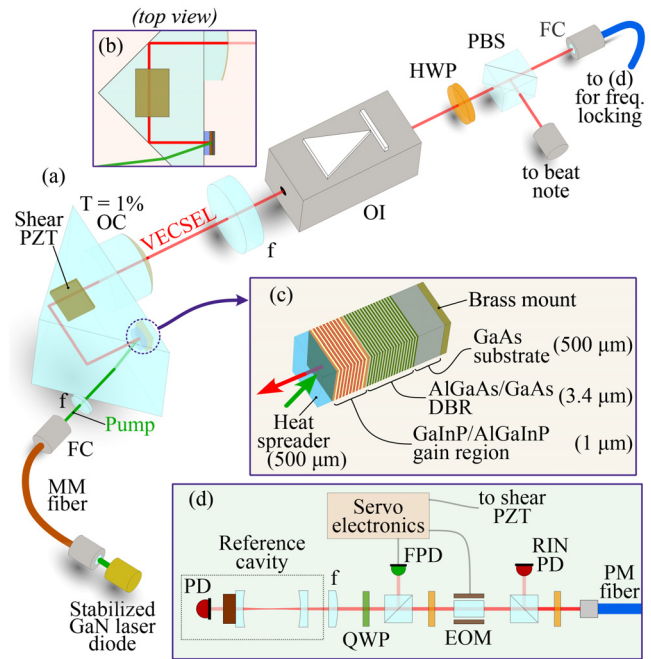


**FIG. 1.** (a) AlGaInP-based monolithic cavity VECSEL experimental apparatus. (b) Total internal reflection VECSEL cavity schematic. (c) AlGaInP-based VECSEL gain structure schematic. (d) Frequency locking setup schematic (when implemented). MM fiber: multimode fiber; FC: fiber coupler; PZT: piezo-electric transducer; OC: output coupler; f: lens; OI: optical isolator; HWP: half-wave plate; PBS: polarizing beam splitter; PD: photodiode; DBR: distributed Bragg reflector; freq.: frequency; PM fiber: polarization maintaining fiber; (F)PD: (fast) photo-detector; RIN: relative intensity noise; EOM: electro-optical modulator; and QWP: quarter-wave plate.

Fig. 2(a)]. In contrast to air-spaced configurations, no intracavity filtering is implemented for wavelength tuning. Instead, the emission wavelength is electronically tunable without mode hopping via the monolithic cavity mount temperature (also affecting the gain
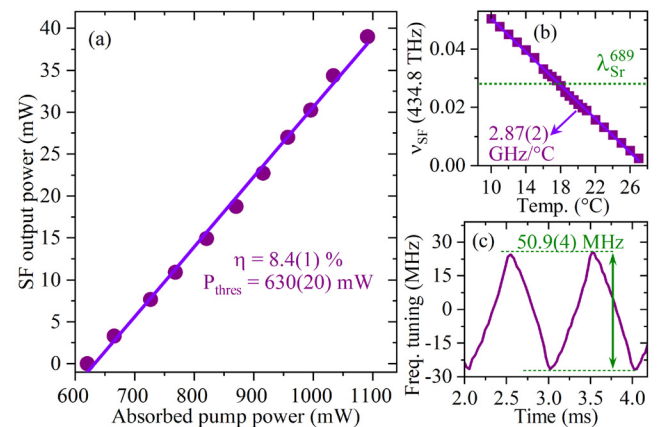


**FIG. 2.** (a) Monolithic cavity VECSEL power transfer. (b) Coarse tuning achieved using the cavity temperature. (c) Fine tuning via the shear PZT measured by sending a sawtooth function directly to the device.

structure temperature), and the shear PZT mounted on the top of prism. The former provides coarse wavelength tuning at a rate of 2.87 (2) GHz/°C, or 3.32(3) pm/°C [see Fig. 2(b)], which directly affects the wavelength stability given that it also controls the VECSEL gain structure temperature. The latter is used for fine wavelength tuning in a frequency span of 50.9(4) GHz, or 81(1) pm [see Fig. 2(c)]. All subsequent noise characterization reported here was measured at the maximum VECSEL output power of 40 mW.

The monolithic cavity VECSEL output beam is collimated and divided using polarization optics for the heterodyne beat note setup and for the noise characterization/locking stage [Fig. 1(d)]. The latter stage is used to frequency stabilize the monolithic cavity VECSEL to a moderately high finesse, air-spaced reference cavity (finesse = 1k and free spectral range = 300 MHz) via the Pound–Drever–Hall technique (EOM modulation = 74 MHz and bandwidth = 500 Hz),[11] with the error signal sent back to the shear PZT mounted on the top of the prism.[16] The overall performance of the VECSEL is characterized in terms of frequency and intensity noise, Allan deviation, and linewidth when the laser is free-running and locked.

First, the relative intensity noise, or RIN [see Fig. 3(a)] is measured to be below −112 and −124 dB/Hz when free-running and locked, respectively, for frequencies between 100 mHz and 1.5 MHz. The low frequency intensity noise is significantly reduced when the laser is locked, but sharp peaks can still be observed between 10 Hz and 7 kHz, related to mechanical, electronic, and pump-injected noise [also shown in Fig. 3(a)], indicating that further improvements in the

mechanical stabilization and pump intensity stabilization are required to lower the RIN noise floor.

A frequency noise power spectral density (FNPSD) was generated using the residual error signal from the servo controller, presented in Fig. 3(b), recorded over a sampling time of 20 s to account for low frequency noise contributions. Similar to the RIN measurements, residual pump intensity noise injected in the VECSEL and mechanical and environmental noise affecting the laser setup and (non-monolithic) pump beam pointing are the main frequency noise components. Also included in Fig. 3(b) is the β-separation line, which is defined as $S_\beta = (8\pi^{-2}\ln2)f$, where f is the Fourier frequency, used to divide the FNPSD into two regions: frequency noise above and below the β-separation line contributing to the central (Gaussian), or laser linewidth, and to the wings (Lorentzian) of the line shape, respectively. The shape of the optical field can be reconstructed via autocorrelation and the Wiener–Khintchine theorem[21] to estimate the linewidth of the monolithic VECSEL, resulting in a FWHM of 830(10) and 480(10) Hz when free-running and locked, respectively, for sampling times of 20 s.

At the time scales (>1 s) presented here, the linewidth can be understood as "integrated," given that different FN components, such as random walk (or $1/f^2$) and flicker-noise (or $1/f$), will be responsible for the broadening of the Gaussian part of the line shape, thus broadening the laser intrinsic, or Lorentzian, linewidth. The Lorentzian contribution is negligible at long time scales but very relevant at more instantaneous scales (<1 μs), where the laser noise spectrum is dominated by white frequency noise,[22] presenting the narrowest achievable spectral purity if all external noise can be suppressed. A narrow Lorentzian linewidth is also desirable in the "integrated" linewidth case given that it will result in negligible contributions to the wings of the laser line shape. The Lorentzian linewidth can be measured from a FNPSD for frequencies far-from-carrier where the $1/f$-noise is no longer relevant, with the noise spectrum dominated by white frequency noise.[22–24] For the monolithic cavity VECSEL presented here, the white noise-only region in the FNPSD measurement [see Fig. 4(b)] is achieved for frequencies above 1 MHz and is maintained for frequencies up to 150 MHz [see Fig. 4(b) inset], resulting in an intrinsic linewidth of 63.5 mHz. This ultra-narrow Lorentzian linewidth is in accordance with the predicted STH limit for VECSEL technology, but might also be affected by the injection of excess electronic noise in the error signal used to generate the FNPSD, drifts and pump noise being injected in the VECSEL cavity out with the correction bandwidth of the intensity stabilization. More precise measurements of the intrinsic linewidth can be performed with higher resolution frequency discriminator systems, such as ultra-high-finesse ultra-stable cavities[5] and Mach–Zehnder interferometers.[22,23] Nevertheless, the monolithic cavity VECSEL performance presented here highlights the potential of this class-A laser technology for the development of ultra-coherent, ultra-low noise laser systems with even narrower free-running linewidths. This kind of performance might enable the use of monolithic-cavity VECSELs for optical coherent and free-space communications,[25] where the signal-to-noise ratio is severely affected by the laser frequency, phase noise performance, and linewidth. In addition, linewidths even closer to the STH linewidth limit, estimated to be ~0.5 mHz, might be achievable with VECSEL technology advantages, including external cavity architecture that reduces the effect of the linewidth enhancement, or Henry, factor in the frequency noise.[22]
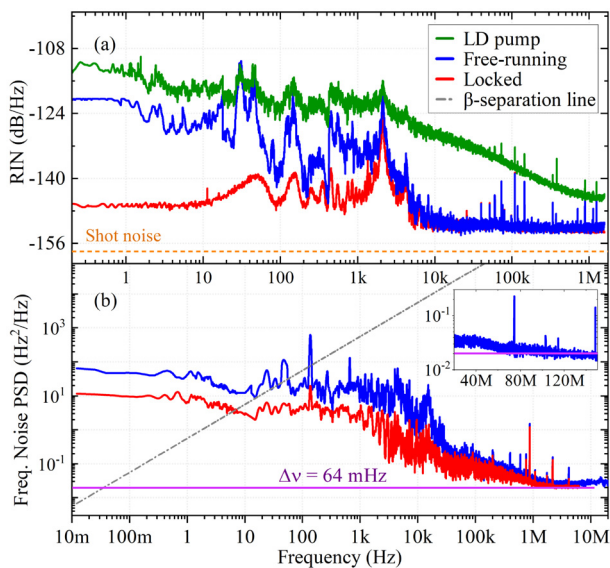


**FIG. 3.** Monolithic VECSEL noise analysis in terms of intensity noise and frequency noise (FN) while free-running (blue) and locked (red). (a) Relative intensity noise, including the monolithic cavity VECSEL shot noise (orange dash) and stabilized laser diode (LD) pump (green) for frequencies below 2 MHz. (b) FN power spectral density (FNPSD), including the β separation line (grey dot-dash), which divides the FNPSD into two regions: high frequency Lorentzian "wings" and the low frequency Gaussian line shape, and a (purple) line indicating the far-from-carrier white-frequency-noise level used to determine the intrinsic linewidth. *Inset*: FNPSD for high frequencies from 20 to 200 MHz, calculated for a sampling time of 400 ns.
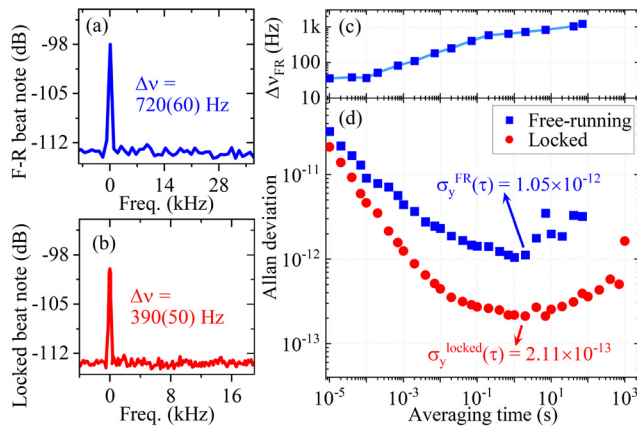
**FIG. 4.** (a) Free-running and (b) locked monolithic cavity VECSEL heterodyne beat note measurement (averaging time of 2 s) against a locked, air-spaced VECSEL at 689 nm with an estimated linewidth of 200 Hz (via the residual error signal measured for a sampling time of 40 s). (c) Heterodyne beat-note full-width at half-maximum vs averaging time. (d) Allan deviation derived from the heterodyne beat note measurement.

In order to characterize the laser frequency stability and validate the monolithic cavity VECSEL linewidth, a heterodyne beat note measurement was performed against a second air-spaced VECSEL at 689 nm with an estimated linewidth of 200 Hz[11] for an averaging time of 40 s. The two lasers had emission wavelength separated by a frequency difference of 300 MHz. The VECSEL beams were then combined on a 50:50 splitting ratio non-polarizing beam splitter and sent to the detection system via a polarization-maintaining fiber, with the resulting radio frequency (RF) beat note peak signal being measured by a fast photodetector (bandwidth 1 GHz), and recorded with an oscilloscope and an electric spectrum analyzer. The beat note peaks for the free-running and locked VECSEL shown in Figs. 4(a) and 4(b), respectively, have full-width at half-maximum of 720(60) and 390(50) Hz, respectively, for an averaging time of 2 s, in good agreement with the estimated spectral width values calculated from the FNPSD for a sampling time of 20 s. It is also important to note that free-running linewidths of 40 Hz, as shown in Fig. 4(c) inset, are measured for shorter averaging times between 10 and 100 µs and then broadened by excess noise and cavity drifts for longer times, maintaining sub-kilohertz linewidth up to time averaging of 10 s.

Finally, the Allan deviation, calculated from the heterodyne beat note data recorded for different ranges of averaging times, was used to measure the frequency stability of the monolithic cavity VECSEL against the reference-cavity-locked, air-spaced VECSEL.[11] While free-running, a frequency stability of $1.05 \times 10^{-12}$ is measured for an averaging time of 1s, staying $< 5 \times 10^{-12}$ for longer times up to 40 s. The locked stability is measured to be $2.11 \times 10^{-13}$ for averaging time of 2 and 7 s. The increase in the Allan deviation for longer averaging times is mainly caused by drifts of the reference and air-spaced VECSEL cavities, which were not compensated for in this frequency stability measurement. Regardless of the frequency stability incremental due to reference cavity drifts and environmental noise, the linewidth and frequency stability performance demonstrated here presents a more stable performance than free-running air-spaced VECSEL counterparts at the same wavelength.[11,14]

In conclusion, we have demonstrated sub-kilohertz linewidth operation of a free-running VECSEL using a GaInP/AlGaInP-based monolithic cavity at 689 nm optically pumped by an intensity-stabilized green diode laser. Free-running and locked linewidth were measured to be 720 Hz (1 s) and 390 Hz (7 s), with a sub-kilohertz free-running linewidth maintained for averaging times up to 40 s. In addition, examination of the FNPSD at high frequencies showed the monolithic cavity VECSEL has an ultra-narrow intrinsic linewidth of 63.5 mHz. Finally, the frequency stability was measured in terms of Allan deviation to be $1.05 \times 10^{-12}$ (1 s) while free-running, which is improved to $2.11 \times 10^{-13}$ (7 s) when active stabilization is implemented. The high-performance and stability presented here can be further improved by reducing the mechanical, electronic, and thermal noise still affecting the overall laser performance, e.g., with better isolation of the prism and increasing pump stability. Increasing the correction bandwidth of the shear PZT in the first instance will allow for tighter frequency locks, resulting in even lower intensity and frequency noise to move further toward the VECSEL fundamental limit. This can be achieved, for example, with further miniaturization of the monolithic cavity geometry and mount design, thus allowing for a higher correction bandwidth while avoiding mount mechanical resonances; by a tighter intensity stabilization of the pump laser to reduce injection of excess pump noise into the VECSEL cavity; and by improving the thermal management of the VECSEL gain structure. Nevertheless, the monolithic cavity VECSEL at 689 nm presented here exceeds the target performance in terms of brightness, intensity and frequency noise, linewidth, and frequency stability required by high precision quantum technology applications, such as neutral Sr optical lattice clocks.

## AUTHOR DECLARATIONS
### Conflict of Interest

The authors have no conflicts to disclose.

### Author Contributions

**P. H. Moriya:** Conceptualization (equal); Data curation (lead); Formal analysis (lead); Funding acquisition (supporting); Investigation (lead); Methodology (equal); Project administration (equal); Resources (equal); Software (lead); Supervision (supporting); Validation (lead); Visualization (lead); Writing – original draft (lead); Writing – review & editing (equal). **M. Lee:** Conceptualization (equal); Methodology (equal); Writing – review & editing (supporting). **J. E. Hastie:** Conceptualization (equal); Funding acquisition (lead); Methodology (equal); Project administration (equal); Resources (lead); Supervision (lead); Validation (supporting); Writing – review & editing (equal).

17 July 2024 08:29:38

## DATA AVAILABILITY

The data that support the findings of this study are openly available in University of Strathclyde KnowledgeBase at https://doi.org/10.15129/d0fa0019-562a-4dab-bfde-392d6864e77e, Ref. 26.

## REFERENCES

[1]S. Falke, N. Lemke, C. Grebing, B. Lipphardt, S. Weyers, V. Gerginov, N. Huntemann, C. Hagemann, A. Al-Masoudi, S. Häfner, S. Vogt, U. Sterr, and C. Lisdat, New J. Phys. **16**, 073023 (2014).

[2]L. Hu, E. L. Wang, L. Salvi, J. N. Tinsley, G. M. Tino, and N. Poli, Classical Quantum Gravity **37**, 1 (2020).

[3]L. Fallani and A. Kastberg, Europhys. Lett. **110**, 53001 (2015).

[4]N. Ohmae, M. Takamoto, Y. Takahashi, M. Kokubun, K. Araki, A. Hinton, I. Ushijima, T. Muramatsu, T. Furumiya, Y. Sakai, N. Moriya, N. Kamiya, K. Fujii, R. Muramatsu, T. Shiimado, and H. Katori, Adv. Quantum Technol. **4**, 2100015 (2021).

[5]C. Qiao, C. Z. Tan, F. C. Hu, L. Couturier, I. Nosske, P. Chen, Y. H. Jiang, B. Zhu, and M. Weidemüller, Appl. Phys. B **125**, 215 (2019).

[6]A. Sottile, E. Damiano, A. Di Lieto, and M. Tonelli, Opt. Lett. **44**, 594 (2019).

[7]A. L. Schawlow and C. H. Townes, Phys. Rev. **112**, 1940 (1958).

[8]C. H. Henry, IEEE J. Quantum Electron. **18**, 259 (1982).

[9]C. Hessenius, N. Terry, M. Fallahi, J. Moloney, and R. Bedford, Opt. Lett. **35**, 3060 (2010).

[10]M. Guina, A. Rantamäki, and A. Härkönen, J. Phys. D: Appl. Phys. **50**, 383001 (2017).

[11]P. H. Moriya, Y. Singh, K. Bongs, and J. E. Hastie, Opt. Express **28**, 15943 (2020).

[12]P. H. Moriya, M. Lee, and J. E. Hastie, Opt. Express **31**, 28018 (2023).

[13]P. Kwee, C. Bogan, K. Danzmann, M. Frede, H. Kim, P. King, J. Pöld, O. Puncken, R. L. Savage, F. Seifert, P. Wessels, L. Winkelmann, and B. Willke, Opt. Express **20**, 10617 (2012).

[14]M. Lee, P. H. Moriya, and J. E. Hastie, Opt. Express **31**, 38786 (2023).

[15]I. Courtillot, A. Quessada-Vial, A. Brusch, D. Kolker, G. D. Rovera, and P. Lemonde, Eur. Phys. J. D **33**, 161 (2005).

[16]E. D. Black, Am. J. Phys. **69**, 79 (2001).

[17]Y. Fan, A. van Rees, P. J. M. van der Slot, J. Mak, R. M. Oldenbeuving, M. Hoekman, D. Geskus, C. G. H. Roeloffzen, and K.-J. Boller, Opt. Express **28**, 21713 (2020).

[18]C. Xiang, J. Guo, W. Jin, L. Wu, J. Peters, W. Xie, L. Chang, B. Shen, H. Wang, Q.-F. Yang, D. Kinghorn, M. Paniccia, K. J. Vahala, P. A. Morton, and J. E. Bowers, Nat. Commun. **12**, 6650 (2021).

[19]G. Lihachev, J. Riemensberger, W. Weng, J. Liu, H. Tian, A. Siddharth, V. Snigirev, V. Shadymov, A. Voloshin, R. N. Wang, J. He, S. A. Bhave, and T. J. Kippenberg, Nat. Commun. **13**, 3522 (2022).

[20]P. H. Moriya, R. Casula, G. A. Chappell, D. C. Parrotta, S. Ranta, H. Kahle, M. Guina, and J. E. Hastie, Opt. Express **29**, 3258 (2021).

[21]G. Di Domenico, S. Schilt, and P. Thomann, Appl. Opt. **49**, 4801 (2010).

[22]M. A. Tran, D. Huang, and J. E. Bowers, APL Photonics **4**, 111101 (2019).

[23]S. Gundavarapu, G. M. Brodnik, M. Puckett, T. Huffman, D. Bose, R. Behunin, J. Wu, T. Qiu, C. Pinho, N. Chauhan, J. Nohava, P. T. Rakich, K. D. Nelson, M. Salit, and D. J. Blumenthal, Nat. Photonics **13**, 60 (2019).

[24]N. Chauhan, A. Isichenko, K. Liu, J. Wang, Q. Zhao, R. O. Behunin, P. T. Rakich, A. M. Jayich, C. Fertig, C. W. Hoyt, and D. J. Blumenthal, Nat. Commun. **12**, 4685 (2021).

[25]A. Kakkar, J. Rodrigo Navarro, R. Schatz, X. Pang, O. Ozolins, A. Udalcovs, H. Louchet, S. Popov, and G. Jacobsen, Sci. Rep. **7**, 844 (2017).

[26]See https://doi.org/10.15129/d0fa0019-562a-4dab-bfde-392d6864e77e for "University of Strathclyde KnowledgeBase."